

A Twisted Ladder: relating the Fe superconductors to the high T_c cuprates

E. Berg¹, S. A. Kivelson¹, and D. J. Scalapino²

¹Department of Physics, Stanford University, Stanford, CA 94305-4045, USA

²Department of Physics, University of California, Santa Barbara, CA 93106-9530, USA

(Dated: February 21, 2024)

We construct a 2-leg ladder model of an Fe-pnictide superconductor and discuss its properties and relationship with the familiar 2-leg cuprate model. Our results suggest that the underlying pairing mechanism for the Fe-pnictide superconductors is similar to that for the cuprates.

An important question has been raised by the discovery of high temperature superconductivity (HTS) in the Fe-pnictides: Is there a single general mechanism of HTS which operates, albeit with material specific differences, in both the Fe-pnictides and the cuprates (and possibly other novel superconductors), or do the cuprates and the Fe-pnictides embody two of possibly many different mechanisms of HTS? This question is complicated by one of the perennial issue of the field: To what extent is it possible to understand the properties of the strongly correlated electron fluid in the Fe-pnictides, the cuprates, and other materials from a weak or strong coupling perspective, given that the materials exhibit some features that appear more natural in one limit and some that are suggestive of the other. The Fe-pnictides, like the cuprates, are likely in the intermediate coupling regime [1–4], which is difficult to treat theoretically.

In the present paper, we introduce a model of a two-leg ladder with an electronic structure chosen to reproduce particular momentum cuts through the Fe-pnictides band structure. We study the magnetic and superconducting properties of this model numerically using the density matrix renormalization group (DMRG) [5] method which allows us to treat the “intermediate coupling” problem essentially exactly. Although the existence of short range, spin gapped, antiferromagnetic correlations in the half-filled two-leg Hubbard ladder and the power-law d -wave-like pairing correlations in the doped ladder were initially unexpected [6], this behavior is now well understood [7–9]. Thus it is not surprising that a two-leg ladder model of the Fe-superconductors exhibits short range antiferromagnetic correlations and power-law pairing. However, it is interesting to see how such a model captures particular aspects of the physical properties of the Fe superconducting materials [10], specifically their spin and pairing correlations.

We find that, in the limit of zero temperature, this model has a diverging superconducting susceptibility with a pair structure of a form which is the quasi-one dimensional version of the structures which have been proposed on the basis of both weak [11–16] and strong [17] coupling calculations for the 2D system. We also find that the dominant magnetic correlations are “stripe-like” with wave vector $(0, \pi)$, reminiscent of the magnetic structure that is seen in the undoped parent compounds

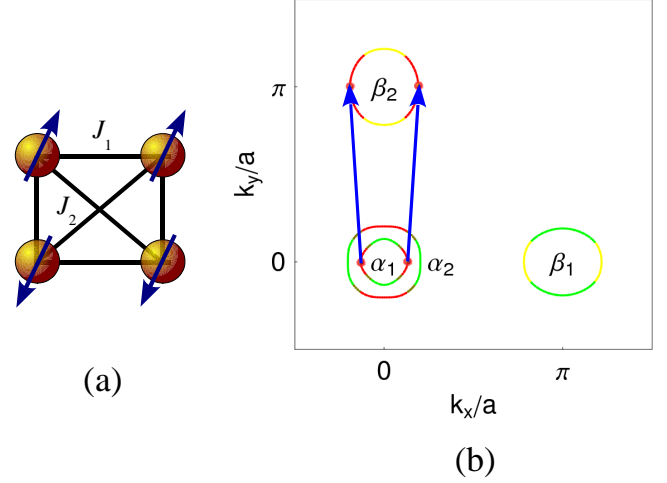


FIG. 1: (a) Heisenberg model showing local Fe spins coupled by comparable nearest neighbor J_1 and next nearest neighbor J_2 exchange couplings. (b) 5-orbital tight binding Fermi surfaces with the main orbital contributions shown by the colors: d_{xz} (red), d_{yz} (green), and d_{xy} (yellow). The arrows illustrate the type of scattering processes which give rise to pairing in the fluctuation exchange calculations.

(and sometimes coexisting with superconductivity) in the Fe-pnictide superconductors. In addition, we show that the Fe-pnictide ladder is a “twisted” version of the two-leg Hubbard ladder. Upon untwisting the ladder, a correspondence is found with the familiar results from cuprate related studies: the superconductivity in the Fe ladder corresponds to “ d -wave-like” correlations in the cuprate Hubbard ladder, and the stripe-like magnetic correlations are transformed into antiferromagnetic correlations with wave vector (π, π) . This supports the idea that there is a single, unified mechanism at work in these two families of HTSs.

As in the case of the cuprates, both strong coupling and weak coupling models have been proposed to account for the magnetic, structural and superconducting properties of the Fe-pnictides. From a strong coupling perspective, the observed magnetic and structural phase transitions and much of the dynamical magnetic structure observed even in the superconducting phase are thought of as arising from frustrated quantum magnetism [18, 19]. Here,

as shown in Fig. 1a, one has for the undoped system a Heisenberg model in which the second-neighbor anti-ferromagnetic interaction, J_2 , is comparable to or larger than the nearest-neighbor exchange interaction, J_1 . For the doped system, one has a $t - J_1 - J_2$ model. Then, as discussed in Ref. [17], a mean-field analysis shows that the dominant pairing channel involves intra-orbital ($d_{xz,\uparrow}, d_{xz,\downarrow}$) and ($d_{yz,\uparrow}, d_{yz,\downarrow}$) pairs, combined to form an A_{1g} superposition. A similar pairing structure was found in Ref. [20] in the large U limit of an exact diagonalization study of a $\sqrt{8} \times \sqrt{8}$ cluster. While both of these studies only took into account the d_{xz} and d_{yz} orbitals, their finding concerning the importance of intra-orbital pairing is relevant to the model we will discuss.

Alternatively, the weak coupling picture begins by considering the energy bands and the Fermi surface. Fig. 1b shows the Fermi surfaces for a five-orbital tight binding fit [16] of a density function theory (DFT) calculation [21], neglecting the effects of dispersion in the third direction, perpendicular to the Fe-pnictide planes. Here the color indicates the relative weights of the 3d (d_{xz} , d_{yz} , d_{xy}) orbitals which form the main contribution to the Bloch wavefunctions on the Fermi surfaces. The d_{xz} and d_{yz} orbitals provide the dominant weight on the hole Fermi surfaces α_1 and α_2 around the Γ point, while on the β_1 and β_2 electron Fermi surfaces one has (d_{yz} , d_{xy}) and (d_{xz} , d_{xy}) contributions, respectively.

From a weak coupling perspective, it is the nesting properties of the α and β Fermi surfaces that give rise to the spin density wave (SDW) instability which accounts for the magnetism of the undoped parent compounds. For the doped system, fluctuation exchange [12, 13, 16, 22, 23] and renormalization group [14, 15] calculations find that magnetic fluctuations near $(\pi, 0)$ and $(0, \pi)$ lead to a pairing instability. In this case, similar to the strong-coupling model, the pairing arises from the type of scattering processes illustrated in Fig. 1b. Here, a $(\mathbf{k} \uparrow, -\mathbf{k} \downarrow)$ pair on the d_{xz} region of the α_1 Fermi surface is scattered by a $\mathbf{Q} = (0, \pi)$ spin fluctuation to a $(\mathbf{Q} + \mathbf{k}' \uparrow, \mathbf{Q} - \mathbf{k}' \downarrow)$ pair on the d_{xz} part of the β_2 Fermi surface. Similar $(\pi, 0)$ processes involving d_{yz} pair scattering occur between α_1 and β_1 .

Thus, both strong-coupling and weak-coupling approaches have been used to describe these materials. However, what is needed is an approach which allows one to treat the intermediate coupling regime. Here, using DMRG, we address this issue for a caricature of the original problem which focuses on the d_{xz} orbital $\alpha_1 - \beta_2$ scattering process for $k_y = 0$ and $k_y = \pi$ states near the Fermi surface. These scattering processes can be described by the two-leg ladder shown in the inset of Fig. 2 with a Hamiltonian given by

$$H = -t_1 \sum_{i,\alpha\sigma} d_{i,\alpha\sigma}^\dagger d_{i+1,\alpha\sigma} - 2t_2 \sum_{i\sigma} d_{i,1\sigma}^\dagger d_{i,2\sigma}$$

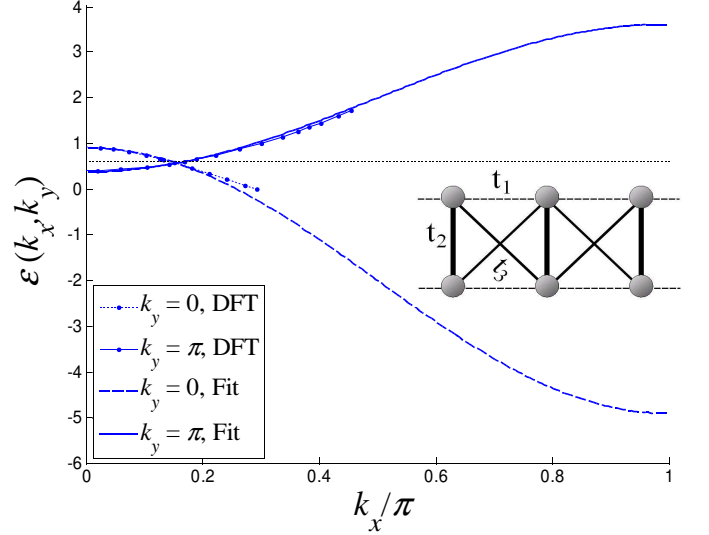


FIG. 2: Band structure $\varepsilon(k_x, k_y)$ of the ladder with $t_1 = -0.32$, $t_2 = 1$ and $t_3 = -0.57$. The solid and dashed curves correspond to $k_y = 0$ and π , respectively. The black dotted line corresponds to the Fermi energy for a filling of one electron per d_{xz} orbital. The dots represent the bands from a DFT calculation [21] for the 2D lattice, cut through $k_y = 0$ and π . The inset shows the ladder with the one electron hopping matrix elements t_1, t_2 and t_3 .

$$-2t_3 \sum_{i\sigma} d_{i,1\sigma}^\dagger d_{i+1,2\sigma} + \text{h.c.} + U \sum_{i,\alpha\sigma} n_{i,\alpha\uparrow} n_{i,\alpha\downarrow}. \quad (1)$$

Here, $\alpha = 1, 2$ is the leg index, $\sigma = \uparrow, \downarrow$ is the spin index, there are leg t_1 , rung t_2 and diagonal t_3 one-electron hopping matrix elements and an on-site Coulomb interaction U . The factors of 2 in front of t_2 and t_3 take into account the periodic boundary conditions transverse to the ladder. The hopping strengths were fitted to the DFT band dispersion of the α_1 and β_2 pockets calculated in Ref. [21], cut through $k_y = 0$ and $k_y = \pi$ near the Fermi surfaces. At these points in momentum space, the Bloch wavefunctions have a d_{xz} character. The parameters we used were $t_1 = -0.32$ and $t_3 = -0.57$, measured in energy units in which $t_2 = 1$. The ladder bandstructure is shown in Fig. 2, where it is compared to the DFT dispersions near the Fermi energy. The dotted line marks the location of the chemical potential for the half-filled, one electron per d_{xz} orbital case. To capture the intermediate coupling aspect of the physics, we will take the onsite Coulomb interaction $U = 3$. This value of the interaction is smaller than the overall bandwidth of the ladder, but larger than the Fermi energies of the hole and electron pockets relative to their values at $k_x = 0$.

DMRG calculations were carried out for a 32×2 system. As expected, there is a spin gap, and the doped system exhibits power-law pairing correlations. At half-filling, in the presence of an externally applied magnetic field on the first site of the lower leg, we find the striped

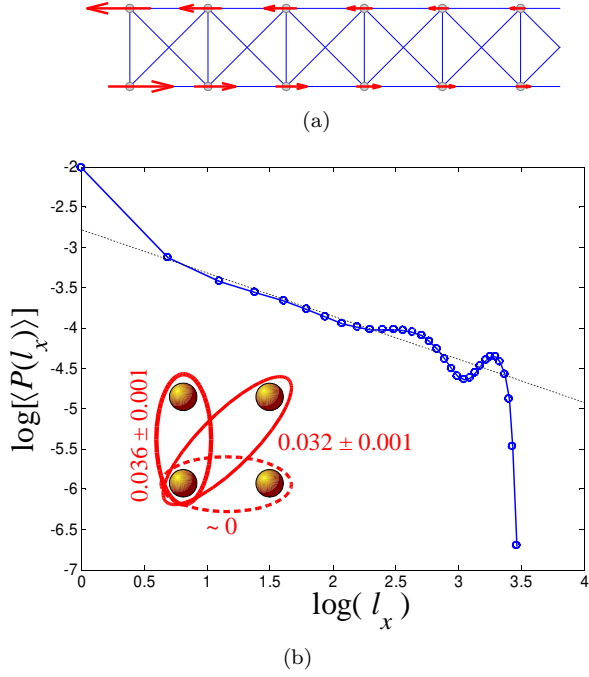


FIG. 3: (a) Spin structure for the undoped ladder, for $U/t_2 = 3$. The lengths of the arrows indicate the measured values of $\langle S^z(l_x) \rangle$ in a calculation in which an external magnetic field has been applied to the lower leftmost site. $\langle S^z(l_x) \rangle$ decays exponentially with a correlation length of about four sites. (b) Pairfield structure for the $\langle n \rangle = 0.94$ doped ladder. Here, a pairfield boundary condition has been applied to a rung on one end of the ladder and the induced rung pairfield $\langle P_l \rangle$ versus l_x is shown on a log-log plot. The amplitude of the singlet pairfield across a rung and along a diagonal at $l_x = 10$ are shown in the inset. The error bars in the pair fields were estimated from the extrapolation of the DMRG truncation error to zero. The pairfield amplitude along a leg is less than 10^{-3} .

spin pattern shown in Fig. 3a. The spin correlations decay exponentially with a correlation length of about four sites and a spin gap $\Delta_s = 0.14$.

For the lightly hole doped case, $\langle n \rangle = 0.94$ (4 holes), we find a spin gap $\Delta_s = 0.07$ and power-law pairfield correlations. Here, a pairfield boundary term

$$H_1 = \Delta_1 (P_1^\dagger + \text{h.c.}), \quad (2)$$

with $\Delta_1 = 0.5$ and

$$P_1^\dagger = (d_{1,1\uparrow}^\dagger d_{1,2\downarrow}^\dagger - d_{1,1\downarrow}^\dagger d_{1,2\uparrow}^\dagger) \quad (3)$$

was added to the Hamiltonian. This acts as a proximity coupling to a rung on the end of the ladder.

The two leg ladder is in a phase with a single gapless charge mode, and the long range correlations are power laws characterized by the Luttinger parameter K_c . For $K_c > \frac{1}{4}$ the superconducting susceptibility is divergent,

and for $K_c > \frac{1}{2}$ it is dominant over the charge density wave susceptibility. In addition, if $K_c > \frac{1}{2}$, the boundary pairing term of Eq. (2) is relevant under a renormalization group flow [24, 25] and the effective boundary condition is described by perfect Andreev reflection. In this case, the induced pair field decays as $|L \tan(\frac{\pi l_x}{2L})|^{-\frac{1}{4K_c}}$, where L is the length of the system [26]. For the stated parameters, the induced expectation value of the rung pair amplitude $\langle P^\dagger(l_x) \rangle = \langle d_{l_x,1\uparrow}^\dagger d_{l_x,2\downarrow}^\dagger - d_{l_x,1\downarrow}^\dagger d_{l_x,2\uparrow}^\dagger \rangle$ was measured throughout the system, and is shown in Fig. 3b on a logarithmic scale. The slope of the curve $\log(\langle P^\dagger(l_x) \rangle)$ vs. $\log(l_x)$ gives $K_c \simeq 0.5$, so the ladder is near the border of the superconducting ($K_c > 0.5$) phase. This conclusion is supported by calculations with longer systems (up to 64×2). For electron doping, we found similar results with slightly smaller values of K_c .

The inset of Fig. 3b shows the amplitude for removing a singlet pair from two sites at a position 10 sites away from the boundary. In order to interpret these results, we perform a BCS mean field treatment of the ladder. In such a treatment, the amplitude for removing a singlet pair from two sites separated by (l_x, l_y) is

$$\begin{aligned} A(l_x, l_y) &\equiv \langle d_{i+l_x, j+l_y\uparrow} d_{i, j\downarrow} - d_{i+l_x, j+l_y\downarrow} d_{i, j\uparrow} \rangle \\ &= \frac{1}{N} \sum_{\mathbf{k}}' \frac{\Delta(\mathbf{k})}{E(\mathbf{k})} e^{i\mathbf{k} \cdot \mathbf{l}}. \end{aligned} \quad (4)$$

Here $E(\mathbf{k}) = \sqrt{[\varepsilon(\mathbf{k}) - \mu]^2 + |\Delta(\mathbf{k})|^2}$, N is the number of sites, and the prime on the \mathbf{k} sum implies that it is cut off when $|\varepsilon(\mathbf{k}) - \mu| > \omega_0$, where ω_0 is a cutoff energy. We assume that the gap function has a simple form in which $\Delta(\mathbf{k})$ is approximately constant for \mathbf{k} in the neighborhood of a given Fermi point, but with a sign change between the $k_y = 0$ and π bands. A reasonable estimate of the relative magnitudes of the gaps on the two bands is obtained by requiring that, due to the strong onsite Coulomb interaction, the onsite pair amplitude vanishes:

$$A(0, 0) \simeq 2 \sum_{k_y=0, \pi} N(0, k_y) \Delta(k_y) \ln \left[\frac{2\omega_0}{\Delta(k_y)} \right] = 0. \quad (5)$$

Here $N(0, k_y)$ and $\Delta(k_y)$ are the density of states at the Fermi energy and the gap function, respectively, of the $k_y = 0$ and π bands. We have assumed that $\Delta(k_y) \ll \omega_0 \ll W$ where W is the bandwidth. From Eqs. (4) and (5), it follows then that the ratio of the amplitude for removing a singlet pair from a diagonal bond to removing it from a rung, $A(1, 1)/A(0, 1)$, is approximately $\frac{1}{2}(\cos k_F(0) + \cos k_F(\pi)) \approx 0.9$. Here $k_F(0)$ and $k_F(\pi)$ are the k_x Fermi momenta for $k_y = 0$ and π , respectively. Similarly, the ratio of the leg to rung amplitude $A(1, 0)/A(0, 1)$ is approximately $\frac{1}{2}(\cos k_F(0) - \cos k_F(\pi)) \approx -0.02$. These amplitude ratios are in overall agreement with the numerical results shown in the inset of Fig. 3b. [$A(1, 0)$ is less than 10^{-3} ,

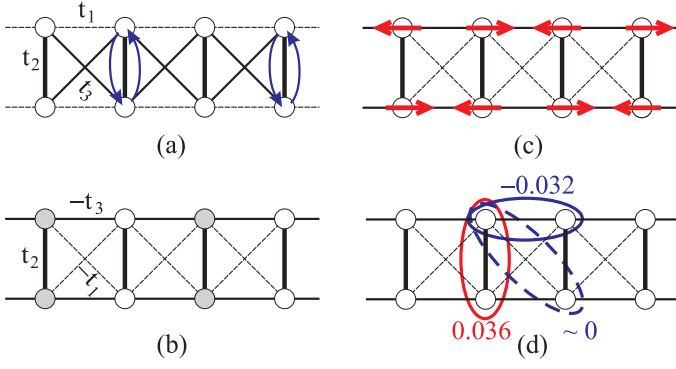


FIG. 4: (a-b) Mapping of the Fe Hubbard ladder, Eq. (1) to the Hubbard ladder used to model the cuprates. (a) Twist every other rung as indicated. (b) Change the sign of the d_{xz} orbital on the shaded sites. (c) The $(0, \pi)$ short range spin correlations of the FeAs ladder (shown in Fig. 3a) become the familiar (π, π) spin correlations of the usual Hubbard ladder after the twists and orbital sign changes shown in (a) and (b). (d) The pairing correlations shown in the inset of Fig. 3b are mapped to the familiar cuprate ladder $d_{x^2-y^2}$ -like pairfield.

which is essentially zero within our numerical accuracy.] The magnitude of the pairing amplitude depends on the strength of the boundary proximity pair field Δ_1 . Note that the rung and diagonal pairfields are in phase with each other. A similar pairfield pattern was found in weak coupling spin-fluctuation calculations [16]. In this case, there were also d_{yz} - d_{yz} orbital pairfield correlations, rotated by 90° . The relative phase of the d_{xz} - d_{xz} and d_{yz} - d_{yz} pairfields determines whether the order parameter has A_{1g} or B_{1g} symmetry. The present study can not address this issue since it lacks the d_{yz} orbitals [27].

At first sight the striped $(0, \pi)$ spin structure of the undoped ladder and the pairing amplitudes of the doped ladder appear different from the (π, π) spin and $d_{x^2-y^2}$ -like correlations familiar for the ladders used to model the cuprates. However, a closer look at the present model reveals that it is in fact identical to that used to model the cuprates.

The mapping between the Fe model we have been discussing and the “usual” two-leg Hubbard ladder is illustrated in Fig. 4. First, every other rung is twisted (Fig. 4a), interchanging the two sites at the ends of the rung and, leading to a ladder having a hopping t_3 along the legs and the weaker hopping t_1 along the diagonals. Then, as illustrated in Fig. 4b, the phases of the orbitals on the shaded sites are changed by -1 . This leads to the usual Hubbard model with $t_{\text{leg}} = -2t_3 = 1.14$, $t_{\text{rung}} = 2t_2 = 2$ and a next-nearest neighbor $t' = -t_1 = 0.32$. After the twist and orbital phase changes, one finds the familiar (π, π) spin correlations shown in Fig. 4c and the $d_{x^2-y^2}$ -like structure for the pairing correlations shown in Fig. 4d.

Finally, we note that the parameters for the FeAs ladder place it near a region of enhanced pairing for the

corresponding Hubbard ladder case [8]. There, it was found that the pairing correlations are enhanced when the parameters are such that the Fermi level is located near the top of the bonding band and the bottom of the anti-bonding band ($t_{\text{rung}}/t_{\text{leg}} \lesssim 2$). The proximity to this point also makes the pairing correlations sensitive to the bandstructure parameters. We have found that while using different bandstructure parameters and a different U does not change the behavior found here qualitatively (e.g., the existence of a spin gap and the pair structure is robust), the strength of the long-range pairing correlations is very sensitive. For instance, for the bandstructure parameters used in the present paper, the pairing correlations are reduced upon increasing the interaction to $U = 4$. For this case, we get $K_c \approx 0.3$. In addition, if we use the band parameters $t_1 = -0.77$, $t_2 = 1$, $t_3 = -0.65$, obtained from a fit to a 2-orbital model [12], and $U = 4.6$, we get a significant enhancement of the pairing correlations, and $K_c \approx 0.75$. The sensitivity of the pairing correlations to the band parameters and to U may be an artifact of the one dimensional nature of the ladder [28]. We believe, however, that the basic superconducting mechanism in the ladder is operative in the FeAs superconductors.

In summary, this analysis began by constructing a ladder model for the Fe-pnictides with hopping parameters chosen to fit DFT calculations. Following the results of the RPA spin-fluctuation calculations and the mean-field $t - J_1 - J_2$ and exact diagonalization studies which indicate that the dominant pairing involves $(0, \pi)$ d_{xz} to d_{xz} and $(\pi, 0)$ d_{yz} to d_{yz} pair scattering processes, only the d_{xz} orbital was kept. Using the DMRG method, we found short range magnetic correlations which mimicked the “striped” $(0, \pi)$ magnetic order in the undoped parent system, and pairing correlations with a structure that agreed with both the weak coupling RPA calculations and the strong coupling results. The Fe-ladder turns out to be simply a twisted version of the usual cuprate Hubbard ladder, with parameters near the regime of enhanced pairing. We believe that this is not an accident but arises from the close connection between the basic physics responsible for high T_c superconductivity in the cuprates and the Fe-pnictides.

Acknowledgement

We thank I. Affleck and S. Raghu for useful discussions. DJS acknowledges the Center for Nanophase Materials Science, which is sponsored at Oak Ridge National Laboratory by the Division of Scientific User Facilities, U.S. Department of Energy and thanks the Stanford Institute of Theoretical Physics for their hospitality. SAK was supported by the NSF through DMR 0758356. EB was supported by the U.S. Department of Energy under contract DE-FG02-06ER46287 through the Geballe Lab-

oratory of Advanced Materials at Stanford University.

-
- [1] K. Haule, J. H. Shim, and G. Kotliar, Phys. Rev. Lett. **100**, 226402 (2008).
 - [2] Q. Si and E. Abrahams, Phys. Rev. Lett. **101**, 076401 (2008).
 - [3] Q. Si, E. Abrahams, J. Dai, and J.-X. Zhu, arXiv: 0901.4112 (2009), unpublished.
 - [4] M.M. Qazilbash, J.J. Hamlin, R.E. Baumbach, L. Zhang, D.J. Singh, M.B. Maple and D.N. Basov, unpublished.
 - [5] S. White, Phys. Rev. Lett. **69**, 2863 (1992).
 - [6] E. Dagatto, J. Riera, and D. Scalapino, Phys. Rev. B. **45**, 5744 (1992).
 - [7] E. Dagatto and T. Rice, Science **271**, 618 (1996).
 - [8] R. Noack, N. Bulut, D. Scalapino, and M. Zacher, Phys. Rev. B **56**, 7162 (1997).
 - [9] L. Balents and M. Fisher, Phys. Rev. B **53**, 12133 (1996).
 - [10] I. Mazin and J. Schmalian, arXiv:0901.4790 (2009), unpublished.
 - [11] I. Mazin, D. Singh, M. Johannes, and M. Du, Phys. Rev. Lett. **101**, 057003 (2008).
 - [12] S. Raghu, X.-L. Qi, C.-X. Liu, D. Scalapino, and S.-C. Zhang, Phys. Rev. B **77**, 220503(R) (2008).
 - [13] K. Kuroki *et. al.*, Phys. Rev. Lett. **102**, 087004 (2008).
 - [14] F. Wang, H. Zhai, Y. Ran, A. Vishwanath, and D. Lee, Phys. Rev. Lett. **102**, 047005 (2009).
 - [15] A. Chubukov, D. Efremov, and I. Eremin, Phys. Rev. B. **78**, 134512 (2008).
 - [16] S. Graser, T. Maier, P. Hirschfeld, and D. Scalapino, New J. Phys. **11**, 025016 (2009).
 - [17] K. Seo, B. A. Bernevig, and J.-P. Hu, Phys. Rev. Lett. **101**, 206404 (2008).
 - [18] C. Fang, H. Yao, W.-F. Tsai, J.-P. Hu, and S. A. Kivelson, Phys. Rev. B **77**, 224509 (2008).
 - [19] C. Xu, Y. Qi, and S. Sachdev, Phys. Rev. B **78**, 134507 (2008).
 - [20] A. Moreo, M. Daghofer, J. A. Riera, and E. Dagotto, Phys. Rev. B. **79**, 134502 (2009).
 - [21] C. Cao, P. J. Hirschfeld, and H.-P. Cheng, Phys. Rev. B **77**, 020506(R) (2008).
 - [22] H. Ikeda, J. Phys. Soc. Jpn **77**, 2008 (2008).
 - [23] Y. Yanagi, Y. Yamakawa, and Y. Ono, J. Phys. Soc. Jpn **77**, 123701 (2008).
 - [24] I. Affleck, J.-S. Caux, and A. Zagoskin, Phys. Rev. B. **62**, 1433 (2000).
 - [25] D. S. A.E. Feiguin, S.R. White and I. Affleck, arXiv:cond-mat/0612636 (2006), unpublished.
 - [26] This result can be derived using an effective Hamiltonian simialr to the one used in: S.R. White, I. Affleck, and D.J. Scalapino, Phys. Rev. B **65**, 165122 (2002), with a Dirichlet boundary condition on one boundary and a Neumann boundary condition on the other (i.e., the superconducting phase is fixed on one edge, and its derivative is zero on the other).
 - [27] The pairing symmetry is determined by the 2D band-structure as well as the intra-orbital Coulomb and exchange interactions. See Ref. [16], and also K. Kuroki, H. Usui, S. Onari, R. Arita, H. Aoki, arXiv: 0904.2612 (2009).
 - [28] For instance, in the ladder there is a square-root singularity of the non-interacting density of states at the van Hove points, which is known to enhance superconductivity when the chemical potential is close to these points. This causes an increased sensitivity to the band parameters and to the doping.